Magnetic anisotropy in $NpRhGa_5$ single crystals

2006 J. Phys.: Condens. Matter 18 411

(http://iopscience.iop.org/0953-8984/18/2/005)

INSTITUTE OF PHYSICS PUBLISHING JOURNAL OF PHYSICS: CONDENSED MATTER

J. Phys.: Condens. Matter **18** (2006) 411–419 doi:10.1088/0953-8984/18/2/005

Magnetic anisotropy in $NpRhGa_5$ single crystals

E Colineau, F Wastin and J Rebizant

European Commission, Joint Research Centre, Institute for Transuranium Elements, Postfach 2340, D-76125 Karlsruhe, Germany

E-mail: colineau@itu.fzk.de

Received 22 August 2005, in final form 23 August 2005
Published 14 December 2005
Online at stacks.iop.org/JPhysCM/18/411

Abstract

We have investigated oriented single crystals of the antiferromagnet $NpRhGa_5$ ($T_N \approx 37$ K) by means of magnetization and specific heat measurements. Strong anisotropy effects are observed: when magnetic fields are applied in the basal plane, the Néel temperature is barely affected. In contrast, in fields applied along the $\boldsymbol{c}$ axis, the second-order transition (magnetic ordering) is shifted to lower temperatures and merges into the first-order transition (reorientation of the magnetic moments). A full mapping of this complex magnetic phase diagram as a function of the temperature (down to 1.6 K), applied magnetic field (up to 9 T) and crystal orientation is presented. This study shows that antiferromagnetic order is more fragile when the magnetic field is applied along the $\boldsymbol{c}$ axis, which is similar to the situation observed for the $NpCoGa_5$ homologue compound.

1. Introduction

The isostructural $AnTGa_5$ series (An = Np, Pu; T = Co, Rh), where either superconductivity [1, 2] or antiferromagnetism [3, 4] is observed, is a layered version of the $AnGa_3$ system. From the structural analogy, a significant anisotropy can be expected and may play an important role in the occurrence of superconductivity in the Pu-based compounds [5].

Strong anisotropy effects are indeed observed in antiferromagnetic ($\boldsymbol{k} = [0\ 0\ 1/2]$) $NpCoGa_5$ [6, 7] where magnetic fields applied in the basal plane barely affect the Néel temperature ($T_N \approx 47$ K), whereas fields applied along the $\boldsymbol{c}$ axis induce a metamagnetic transition to an aligned ferromagnet ($B_c = 4.5$ T at $T = 5$ K). $NpCoGa_5$ carries an ordered magnetic moment $\mu_{Np} \approx 0.84\ \mu_B$ pointing along the $\boldsymbol{c}$ axis. The Sommerfeld specific heat coefficient, $\gamma = 64$ mJ mol^{-1} K^{-2}, is moderately enhanced.

$NpRhGa_5$ develops type I antiferromagnetic order ($\boldsymbol{k} = [0\ 0\ 1/2]$) below $T_N = 37$ K and undergoes a second magnetic transition—corresponding to the reorientation of the magnetic moments from the $\boldsymbol{c}$ axis to the basal plane—at $T^* = 32$ K, as evidenced by magnetization, resistivity, specific heat [4, 8], ^{237}Np Mössbauer [4] and neutron diffraction data [9]. Mössbauer results indicate the occurrence of a Np^{3+} charge state and an ordered Np moment of 0.96 μ_B.

The effective moment is found to be $\mu_{\rm eff} \approx 1.4\,\mu_{\rm B}$ and the Sommerfeld γ coefficient amounts to 50(20) mJ mol^{-1} K^{-2}. $NpNiGa_5$ orders ferromagnetically with a Curie temperature $T_{\rm C} = 30$ K and an additional antiferromagnetic component appears below $T^* = 18$ K [8, 9]. The specific heat coefficient $\gamma \sim 100$ mJ mol^{-1} K^{-2} is the largest in $NpTGa_5$ systems. $NpFeGa_5$ orders antiferromagnetically at $T_{\rm N} = 118$ K and undergoes a second transition at $T^* = 78$ K [8, 9]. The Np magnetic moments are aligned along the $\boldsymbol{a}$ axis and it should be noted that Fe also carries an ordered magnetic moment. The γ coefficient ($\sim$30 mJ mol^{-1} K^{-2}) is the lowest in the $NpTGa_5$ series.

From their crystallographic symmetry, $AnTGa_5$ compounds are expected to display a quasi-bi-dimensional anisotropy. Indeed such anisotropic properties are observed in the magnetism of $NpCoGa_5$ [6, 7] and in the superconductivity of $PuRhGa_5$ [10]. The situation is less clear for $PuCoGa_5$ [11] and $NpRhGa_5$ [8], mainly due to the limited range of experimental magnetic fields investigated.

In this study, we have made measurements on oriented single crystals of $NpRhGa_5$ down to 1.6 K and have extended the investigation of the anisotropic behaviour of magnetism in $NpRhGa_5$ up to 7 T for magnetization measurements and up to 9 T for specific heat measurements. The range 5–9 T appears to be crucial, as a magnetic field of $\sim$7 T applied along the $\boldsymbol{c}$ axis completely destroys the higher temperature antiferromagnetic phase.

2. Experimental details

Single crystals of $NpRhGa_5$ were grown by the Ga flux method [12] and characterized by x-ray diffraction, scanning electron microscope and EDX analyses.

The magnetization measurements were carried out on 25.78 mg and 32.27 mg single-crystalline oriented ($\boldsymbol{H} \parallel \boldsymbol{a}$ and $\boldsymbol{H} \parallel \boldsymbol{c}$ axis) samples using a Quantum Design SQUID (MPMS-7) machine from 300 K down to 2 K and in fields up to 7 T.

The specific heat experiments were performed using 19.40 mg and 9.35 mg single-crystalline oriented ($\boldsymbol{H} \parallel \boldsymbol{a}$ and $\boldsymbol{H} \parallel \boldsymbol{c}$ axis) samples by the relaxation method in a Quantum Design PPMS-9 within the temperature range 1.6–300 K and in magnetic fields up to 9 T. In zero magnetic fields, the specific heat curves $C_p(T)$ are identical (within experimental accuracy) for the two orientations.

3. Experimental results

3.1. Magnetization

The thermal dependence of the magnetic susceptibility with a magnetic field of 2 T aligned along either the $\boldsymbol{a}$ or the $\boldsymbol{c}$ axis is shown in figure 1(a). In agreement with previous investigations [4, 8], the onset of antiferromagnetic order is observed below $T_{\rm N} = 35.8(2)$ K, followed by a second magnetic transition at $T^* = 32.2(2)$ K, attributed to a reorientation of the magnetic moments. The insets of figure 1 show both transitions observed, for $\boldsymbol{H} \parallel \boldsymbol{a}$ and $\boldsymbol{H} \parallel \boldsymbol{c}$. The Néel temperature is revealed by a local maximum in the susceptibility for $\boldsymbol{H} \parallel \boldsymbol{a}$ and by a maximum in the susceptibility thermal derivative for $\boldsymbol{H} \parallel \boldsymbol{c}$ (see [13] and the next section). The moment reorientation temperature T^* is determined as the middle point of the susceptibility jump which is rather sharp and suggests a first-order transition. The insets also show M/H obtained at higher fields (5 and 7 T). When the magnetic field is applied along the $\boldsymbol{a}$ direction, its magnitude has almost no influence on the magnetization. In contrast, fields applied along the $\boldsymbol{c}$ axis dramatically affect the Néel and reorientation temperatures: $T_{\rm N}$ shifts to lower temperatures whereas T^* shifts to higher temperatures. The two transitions finally overlap in a field around 7 T and at 33 K.

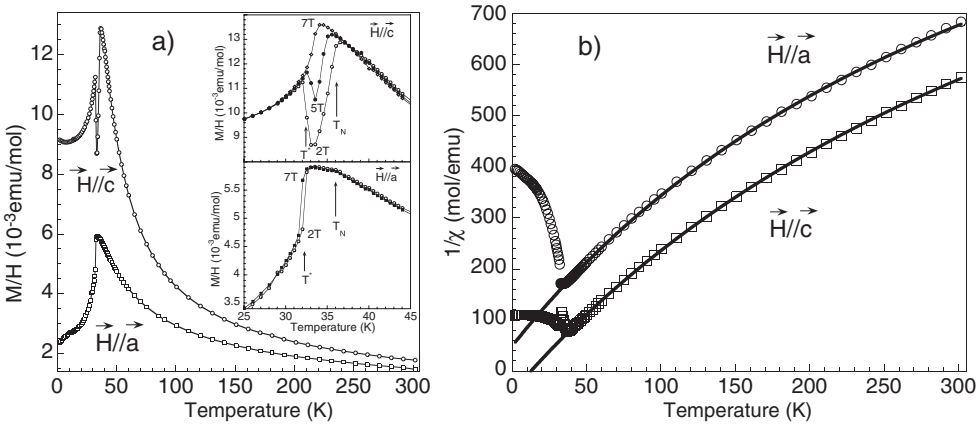

Figure 1. (a) Magnetization in 2 T of $NpRhGa_5$ single crystals with magnetic fields applied along the $\boldsymbol{a}$ and $\boldsymbol{c}$ axes. The insets show the transitions T_N and T^* for both orientations, in different magnetic fields (2 and 7 T, plus 5 T for $\boldsymbol{H} \parallel \boldsymbol{c}$). (b) Inverse magnetic susceptibility of $NpRhGa_5$ with $\boldsymbol{H} \parallel \boldsymbol{a}$ and $\boldsymbol{H} \parallel \boldsymbol{c}$. The symbols represent the experimental points and the solid lines the modified Curie–Weiss fits over the whole paramagnetic domain investigated.

In the paramagnetic state, the magnetic susceptibility can be accounted by a modified Curie–Weiss law (figure 1(b)):

$$\chi = \chi_0 + C/(T - \theta_p) \tag{1}$$

from which the effective moments $\mu_{eff} \approx 1.42\ \mu_B$ and $\mu_{eff} \approx 1.58\ \mu_B$, the paramagnetic Curie temperatures $\theta_p \approx -12.9$ K and $\theta_p \approx 12.5$ K and the constant terms $\chi_0 \approx 667 \times 10^{-6}$ emu mol^{-1} and $\chi_0 \approx 665 \times 10^{-6}$ emu mol^{-1} are inferred for $\boldsymbol{H} \parallel \boldsymbol{a}$ and $\boldsymbol{H} \parallel \boldsymbol{c}$, respectively.

The values of the effective moment are strongly reduced compared to the free ion case and the interaction temperatures, either positive or negative, reveal competitive ferromagnetic and antiferromagnetic interactions. Note that Aoki *et al* [8] reported effective moments closer to the Np^{3+} free ion value (2.75 μ_B in intermediate coupling), obtained by adjusting the linear part of their experimental data, between 260 and 300 K, with a pure Curie–Weiss law. This approach leads to negative paramagnetic Curie temperatures with very high absolute values (-129, -245 and -235 K for $\boldsymbol{H} \parallel$ [001], [100] and [110] respectively). The limited range of temperature, in both experiments, prevents us from definitively assessing the two approaches and high temperature measurements would be necessary.

3.2. Specific heat

The general thermal dependence of the specific heat is represented in figure 2. At high temperature, C_p saturates around 177 J mol^{-1} K^{-1} (at 300 K), very close to the value expected from Dulong and Petit's law [14]:

$$C_p = 3nN_A k_B \approx 175\ \text{J mol}^{-1}\ \text{K}^{-1} \tag{2}$$

with n the number of atoms per molecule, N_A the Avogadro constant and k_B the Boltzmann constant.

A lambda-type peak (see later in this section) can be observed at the Néel temperature but the most remarkable feature here is the very sharp and intense peak at T^* that clearly reflects the first-order character of the second magnetic transition. The inset of figure 2 shows the low

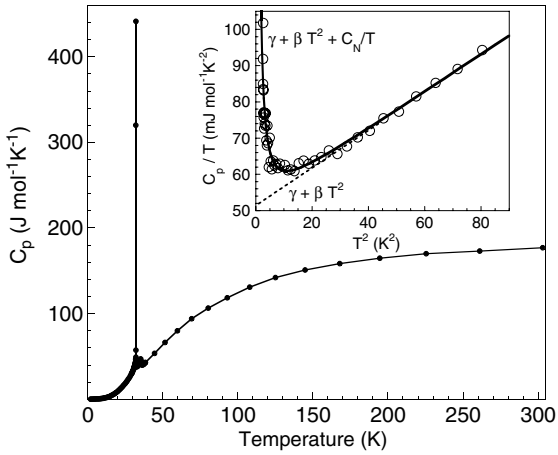

Figure 2. Specific heat of $NpRhGa_5$ versus temperature over the whole temperature range investigated. The inset shows the low temperature part of C_p/T (open symbols) down to 1.6 K and its fit (solid line), taking into account the electronic (γ), phononic (βT^2) and nuclear (C_N/T) contributions. The dashed line shows the extrapolated γ value of from the linear part of the curve.

temperature part of C_p/T versus T^2. Below $T \sim 10$ K, the specific heat can be accounted for by the linear law

$$C_p/T = \gamma + \beta T^2 \tag{3}$$

that reflects the electronic and phononic contributions and yields $\gamma = 51$ mJ mol^{-1} K^{-2}, which is rather close to the value obtained for $NpCoGa_5$ (64 mJ mol^{-1} K^{-2} [3]) and confirms the previous values inferred from polycrystalline [4] and single-crystalline measurements [8]. The value of $\beta = 0.55$ mJ mol^{-1} K^{-4} allows a rough estimate of the Debye temperature $\theta_D \approx 152$ K. Like for $NpCoGa_5$, a sharp upturn is observed at the lowest temperatures (below $\sim$3 K) that is attributed to a nuclear hyperfine Schottky term C_N due to the splitting of the nuclear ground state level ($I = 5/2$) of the ^{237}Np nuclei by the hyperfine magnetic field. In our case, the nuclear contribution C_N can be approximated by the formula [15]

$$C_N = R/3(\mu H_{hf}/k_B I)^2 I(I+1)/T^2 \tag{4}$$

with R the molar gas constant, k_B the Boltzmann constant, μ the nuclear moment of the ^{237}Np ground state (2.5 μ_N), I the nuclear spin of the ^{237}Np ground state (5/2) and H_{hf} the hyperfine magnetic field measured by Mössbauer spectroscopy [4]. The inset of figure 2 shows that the thus calculated $C_N(T)$ perfectly fits with the experimental data down to 1.6 K.

Figure 3 shows the $C_p/T(T)$ curve of $NpRhGa_5$ and $URhGa_5$. The latter is a non-magnetic compound with $\gamma = 13(1)$ mJ mol^{-1} K^{-2} and can be used to account for the phonon contribution in the specific heat of $NpRhGa_5$. The magnetic specific heat of $NpRhGa_5$ is obtained from

$$C_{mag}^{NpRhGa_5} = C_{Total}^{NpRhGa_5} - \gamma^{NpRhGa_5} - (C_{Total}^{URhGa_5} - \gamma^{URhGa_5} T). \tag{5}$$

By thermal integration, we then obtain a magnetic entropy $S_{mag}(T)$ (inset of figure 3) that is close to $R \ln 2$ at T_N. The clear discontinuity observed at T^* corresponds to the first-order transition mentioned before.

The magnetic specific heat is theoretically proportional to the derivative of the magnetic susceptibility [13]:

$$C_{mag}(T) \approx A\, \mathrm{d}[T\chi_{\parallel}(T)]/\mathrm{d}T. \tag{6}$$

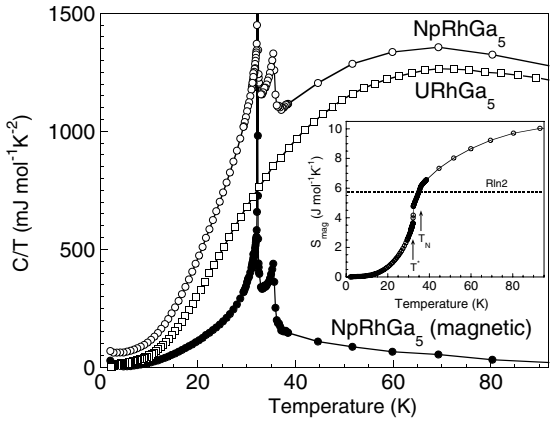

Figure 3. Specific heat of $NpRhGa_5$ (open circles) versus temperature. The curve obtained for non-magnetic $URhGa_5$ (open squares) is shown for comparison and is used to account for the phonon contribution in $NpRhGa_5$. The full circles represent the magnetic contribution to the specific heat for $NpRhGa_5$, obtained by subtracting the phonon and electron contributions (see the text). The inset shows the magnetic entropy of $NpRhGa_5$. The value of $R \ln 2$ (dashed line) is indicated for comparison.

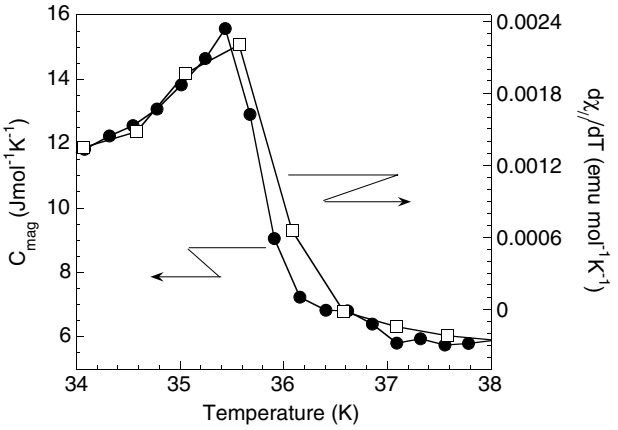

Figure 4. Magnetic specific heat (full circles) and first thermal derivative of the magnetic susceptibility ($\boldsymbol{H} \parallel \boldsymbol{c}$) (open squares) around the Néel temperature defined from the maximum of both curves.

Figure 4 shows that our experimental curves for $C_{\mathrm{mag}}(T)$ and $\mathrm{d}\chi_{\parallel}/\mathrm{d}T$ ($\boldsymbol{H} \parallel \boldsymbol{c}$) around the Néel temperature display exactly the same behaviour. This demonstrates the validity of taking T_{N} at the derivative maximum of the magnetic susceptibility instead of the susceptibility maximum, as mentioned in the previous section.

Figure 5(a) shows the in-field specific heat of $NpRhGa_5$ around T_{N} and T^* for $\boldsymbol{H} \parallel \boldsymbol{a}$. The second-order peak at T_{N} is almost unaffected by magnetic fields up to 9 T, whereas the first-order peak at T^* is slightly (and monotonically) shifted to lower temperatures (from 32.2 K in zero field down to 31.7 K at 9 T).

Figure 5(b) shows the same measurements performed with $\boldsymbol{H} \parallel \boldsymbol{c}$. In this case, the peak at T_{N} is significantly shifted to lower temperatures by magnetic fields, whereas the peak at T^* is

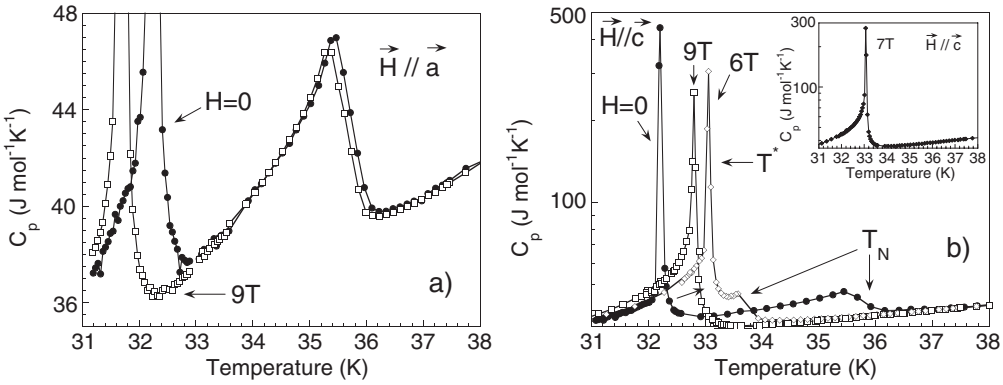

Figure 5. (a) Specific heat around T_N and T^* in different magnetic fields applied along the $\boldsymbol{a}$ axis; (b) specific heat around T_N and T^* in different magnetic fields applied along the $\boldsymbol{c}$ axis. Notice the shift of both T_N and T^*. The latter first shifts upwards between 0 and 6 T, then downwards between 6 and 9 T. T_N merges into T^* at 7 T (see the inset).

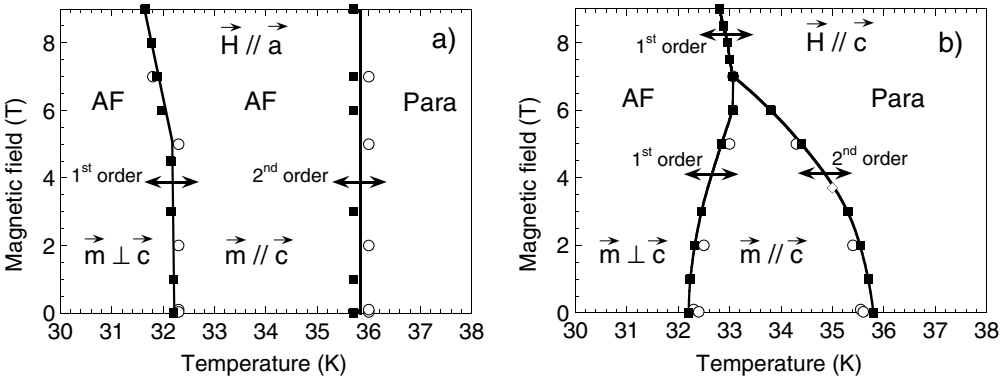

Figure 6. (a) Magnetic phase diagram of $NpRhGa_5$ when the magnetic field is applied along the $\boldsymbol{a}$ axis. T_N and T^* are not significantly affected up to 9 and 5 T, respectively. Above 5 T, T^* shifts linearly to lower temperatures; (b) magnetic phase diagram of $NpRhGa_5$ when the magnetic field is applied along the $\boldsymbol{c}$ axis. The $\boldsymbol{m} \parallel \boldsymbol{c}$ phase is reduced on both sides (T_N decreases and T^* increases) by increasing field and vanishes at 7 T. Further increase of the magnetic field slightly decreases T_N.

shifted to higher temperatures by magnetic fields. The two peaks finally merge at 33 K in a field of 7 T. The resulting peak keeps a first-order character but slightly shifts to lower temperatures on further increasing the magnetic field up to 9 T. We conclude that the 'low temperature' phase grows at the expense of the 'high temperature' phase until the latter vanishes and is then directly affected by the decrease of the Néel temperature with increasing field. These features are in good agreement with magnetic susceptibility measurements and lead to the magnetic phase diagrams presented in figures 6(a) ($\boldsymbol{H} \parallel \boldsymbol{a}$) and 6(b) ($\boldsymbol{H} \parallel \boldsymbol{c}$).

The direction of the magnetic moments in the different phases, as inferred from Mössbauer spectroscopy [4], is also mentioned. From figures 6(a) and (b), it is shown that applying the magnetic field in the basal plane does not affect the 'high temperature' magnetic structure ($\boldsymbol{m} \parallel \boldsymbol{c}$), which remains stable in fields up to 9 T. In contrast, applying the field along the $\boldsymbol{c}$ axis destabilizes this magnetic structure, which collapses above 7 T to the benefit of both

the paramagnetic and the 'low temperature' ($\boldsymbol{m} \perp \boldsymbol{c}$) phases. This suggests that the energy is minimized when the magnetic moments align perpendicular to the applied magnetic field, which is not unusual for antiferromagnets.

4. Discussion

The magnetic phase diagram of $NpRhGa_5$ (figures 6(a) and (b)) displays some strong analogies with that of $NpCoGa_5$ [3, 7], but also some marked differences.

Both compounds order antiferromagnetically with magnetic moments aligned along the $\boldsymbol{c}$ axis and a propagation vector $\boldsymbol{k} = [0\ 0\ 1/2]$. Magnetic fields up to 9 T applied in the basal plane do not affect this antiferromagnetic structure, whereas the application of relatively low magnetic fields (4.5 and 7 T) along the $\boldsymbol{c}$ axis destroys this antiferromagnetic phase in $NpCoGa_5$ and $NpRhGa_5$, respectively.

In contrast to the case for $NpCoGa_5$, this antiferromagnetic structure with $\boldsymbol{m} \parallel \boldsymbol{c}$ does not represent the low temperature phase of $NpRhGa_5$. The latter undergoes a second magnetic transition, about 4 K below the Néel temperature, which is first order and consists of the rotation of the magnetic moments from along the $\boldsymbol{c}$ axis into the basal plane. According to recent theoretical calculations [16], such a thermally induced spin-flip transition indicates itinerant antiferromagnetism and negligible crystal field.

Interestingly, all magnetically ordered $UTGa_5$ compounds (T = Ni, Pd, Pt) display magnetic moments oriented along the $\boldsymbol{c}$ axis, with different wavevectors in $UPdGa_5$ and $UPtGa_5$ ($\boldsymbol{k} = [0\,0\,1/2]$) on the one hand and $UNiGa_5$ ($\boldsymbol{k} = [1/2\,1/2\,1/2]$) on the other hand [17]. In the neptunium series, the situation is more complex, as several magnetic structures are observed: $NpCoGa_5$ ($\boldsymbol{m} \parallel \boldsymbol{c}$, $\boldsymbol{k} = [0\ 0\ 1/2]$), $NpRhGa_5$ ($\boldsymbol{m} \parallel \boldsymbol{c}$ and $\boldsymbol{m} \perp \boldsymbol{c}$, $\boldsymbol{k} = [0\ 0\ 1/2]$), $NpFeGa_5$ ($\boldsymbol{m} \perp \boldsymbol{c} = [1/2\ 1/2\ 0]$) are antiferromagnetic and $NpNiGa_5$ exhibits both ferromagnetic and canted antiferromagnet structures [7, 9]. Onishi and Hotta [18] have examined the role of the orbital degree of freedom in the magnetic structure of $NpTGa_5$ compounds, on the basis of the j–j coupling scheme already used by the authors for $UTGa_5$ and $PuTGa_5$ compounds [19]. However, the understanding of the complexity and diversity of magnetic structures and phase diagrams in $NpTGa_5$ systems still requires further experimental and theoretical work. It is in particular not yet fully established whether the 5f electrons should be considered as localized or itinerant, although the latter picture is supported by many experimental hints like reduced magnetic moments compared to the free ion case, enhanced γ values, Mössbauer isomer shift [3, 4] and recent dHvA experiments and band calculations [20].

It is interesting to note that T = Co and Rh correspond to the only neptunium $NpTGa_5$ compounds found so far with a propagation vector $\boldsymbol{k} = [0\ 0\ 1/2]$ and to the only superconducting $PuTGa_5$ systems. Adopting the hypothesis that superconductivity is, in the latter, mediated by magnetic interactions [5, 21], a 'set' of favourable parameters like a $\boldsymbol{k} = [0\ 0\ 1/2]$ wavevector for antiferromagnetic fluctuations, the crystallographic structure (in particular the tetragonality c/a ratio [5]) and the electron count [22], seem to be necessary to tune the electronic parameters to optimal values for superconductivity. Although pertinent, these criteria taken independently are not sufficient for predicting the occurrence of superconductivity, as exceptions exist in each case. In particular, no superconducting Np-based compound has been found yet, in any system at all. Actually Np compounds are generally the magnetically ordered equivalent of their U or Pu superconducting counterparts.

Similarly to the situation observed for the $NpCoGa_5$ homologue compound [6, 7], the present study shows that antiferromagnetic order is more fragile in $NpRhGa_5$ when the magnetic field is applied along the $\boldsymbol{c}$ axis. It is worth comparing this to the situation for $PuCoGa_5$ [11] and $PuRhGa_5$ [10] where superconductivity is also more fragile in magnetic

fields applied along the c axis. Such an analogy, together with the concomitant higher Néel and critical temperatures in the cobalt $NpCoGa_5$ and $PuCoGa_5$ compounds compared to the rhodium $NpRhGa_5$ and $PuRhGa_5$ compounds, indicates an empirical link between magnetic interactions and superconductivity in the actinide 1:1:5 systems.

5. Conclusion

The full magnetic phase diagrams of $NpRhGa_5$ in the temperature range 1.6–300 K and up to 9 T have been established along the a and c axes by means of magnetization and specific heat measurements on oriented single crystals. They reveal a strong magnetic anisotropy and the first-order character of the magnetic transition occurring at $T^* \approx 32$ K. The antiferromagnetism is found to be more fragile when the magnetic field is applied along the c axis, which is similar to the situation observed for $NpCoGa_5$ and analogous to the field behaviour of the superconductivity in $PuRhGa_5$ and $PuCoGa_5$. From the empirical analogy with the An series and consistency within the T series of the $AnTGa_5$ system, a global picture is emerging that supports magnetically mediated superconductivity in $PuTGa_5$ compounds. Further efforts, both experimental and theoretical, on $AnTGa_5$ compounds should allow progress in the understanding of these complex systems.

Acknowledgments

The authors are grateful to D Aoki, Y Homma, F Honda, K Kaneko, Y Haga, N Metoki and G H Lander for fruitful discussions. The high purity Np metals required for the fabrication of the compound were made available through a loan agreement between Lawrence Livermore National Laboratory and ITU, in the framework of a collaboration involving LLNL, Los Alamos National Laboratory, and the US Department of Energy.

References

[1] Sarrao J L, Morales L A, Thompson J D, Scott B L, Stewart G R, Wastin F, Rebizant J, Boulet P, Colineau E and Lander G H 2002 *Nature* **420** 297–9
[2] Wastin F, Boulet P, Rebizant J, Colineau E and Lander G H 2003 *J. Phys.: Condens. Matter* **15** S2279–85
[3] Colineau E, Javorský P, Boulet P, Wastin F, Griveau J C, Rebizant J, Sanchez J P and Stewart G R 2004 *Phys. Rev.* B **69** 184411
[4] Colineau E, Wastin F, Boulet P, Javorský P, Rebizant J and Sanchez J P 2005 *J. Alloys Compounds* **386** 57
[5] Bauer E D, Thompson J D, Sarrao J L, Morales L A, Wastin F, Rebizant J, Griveau J C, Javorský P, Boulet P, Colineau E, Lander G H and Stewart G R 2004 *Phys. Rev. Lett.* **93** 147005
[6] Aoki D, Homma Y, Shiokawa Y, Yamamoto E, Nakamura A, Haga Y, Settai R, Takeuchi T and Onuki Y 2004 *J. Phys. Soc. Japan* **73** 1665
[7] Metoki N, Kaneko K, Colineau E, Javorský P, Aoki D, Homma Y, Boulet P, Wastin F, Shiokawa Y, Bernhoeft N, Yamamoto E, Onuki Y, Rebizant J and Lander G H 2005 *Phys. Rev.* B **72** 014460
[8] Aoki D, Homma Y, Shiokawa Y, Sakai H, Yamamoto E, Nakamura A, Haga Y, Settai R and Onuki Y 2005 *J. Phys. Soc. Japan* **74** 2323–31
[9] Honda F, Metoki N, Aoki D, Homma Y, Yamamoto E, Onuki Y and Shiokawa Y 2005 *Physica* B **359–361** 1147
[10] Haga Y, Aoki D, Matsuda T D, Nakajima K, Arai Y, Yamamoto E, Nakamura A, Homma Y, Shiokawa Y and Onuki Y 2005 *J. Phys. Soc. Japan* **74** 1698
[11] Sarrao J L, Bauer E D, Morales L A and Thompson J D 2005 *Physica* B **359–361** 1144
[12] Moshopoulou E G, Fisk Z, Sarrao J L and Thompson J D 2001 *J. Solid State Chem.* **158** 25
[13] Fisher M E 1962 *Phil. Mag.* **7** 1731
[14] Dulong P and Petit A T 1819 *Ann. Chim. Phys.* **10** 395
[15] Lounasmaa O V 1967 *Hyperfine Interactions* ed A J Freeman and R B Frankel (New York: Academic)
[16] Varelogiannis G 2003 *Phys. Rev. Lett.* **91** 117201

[17] Kaneko K, Metoki N, Bernhoeft N, Lander G H, Ishii Y, Ikeda S, Tokiwa Y, Haga Y and Onuki Y 2003 *Phys. Rev.* B **68** 214419
[18] Onishi H and Hotta T 2004 *New J. Phys.* **6** 193
[19] Hotta T and Ueda K 2003 *Phys. Rev.* B **67** 104518
[20] Aoki D, Yamagami H, Homma Y, Shiokawa Y, Yamamoto E, Nakamura A, Haga Y, Settai R and Onuki Y 2005 *J. Phys.: Condens. Matter* **17** L169–75
[21] Curro N J, Caldwell T, Bauer E D, Morales L A, Graf M J, Bang Y, Balatsky A V, Thompson J D and Sarrao J L 2005 *Nature* **434** 622
[22] Boulet P, Colineau E, Wastin F, Rebizant J, Javorský P, Lander G H and Thompson J D 2005 *Phys. Rev.* B **72** 104508 (*Preprint* BB10077)